Global Molecular and Morphological Effects of 24-Hour Chromium(VI) Exposure on *Shewanella oneidensis* MR-1

Karuna Chourey,[1] Melissa R. Thompson,[2,3] Jennifer Morrell-Falvey,[4] Nathan C. VerBerkmoes,[2] Steven D. Brown,[1] Manesh Shah,[4] Jizhong Zhou,[5] Mitchel Doktycz,[4] Robert L. Hettich,[2] and Dorothea K. Thompson[6]*

Environmental Sciences Division, Oak Ridge National Laboratory, Oak Ridge, Tennessee 37831[1]; Chemical Sciences Division, Oak Ridge National Laboratory, Oak Ridge, Tennessee 37831[2]; Graduate School of Genome Science and Technology, University of Tennessee-Oak Ridge National Laboratory, Oak Ridge, Tennessee 37830[3]; Life Sciences Division, Oak Ridge National Laboratory, Oak Ridge, Tennessee 37831[4]; Institute for Environmental Genomics and Department of Botany and Microbiology, University of Oklahoma, Norman, Oklahoma 73019[5]; and Department of Biological Sciences, Purdue University, West Lafayette, Indiana 47907[6]

The biological impact of 24-h ("chronic") chromium(VI) [Cr(VI) or chromate] exposure on *Shewanella oneidensis* MR-1 was assessed by analyzing cellular morphology as well as genome-wide differential gene and protein expression profiles. Cells challenged aerobically with an initial chromate concentration of 0.3 mM in complex growth medium were compared to untreated control cells grown in the absence of chromate. At the 24-h time point at which cells were harvested for transcriptome and proteome analyses, no residual Cr(VI) was detected in the culture supernatant, thus suggesting the complete uptake and/or reduction of this metal by cells. In contrast to the untreated control cells, Cr(VI)-exposed cells formed apparently aseptate, nonmotile filaments that tended to aggregate. Transcriptome profiling and mass spectrometry-based proteomic characterization revealed that the principal molecular response to 24-h Cr(VI) exposure was the induction of prophage-related genes and their encoded products as well as a number of functionally undefined hypothetical genes that were located within the integrated phage regions of the MR-1 genome. In addition, genes with annotated functions in DNA metabolism, cell division, biosynthesis and degradation of the murein (peptidoglycan) sacculus, membrane response, and general environmental stress protection were upregulated, while genes encoding chemotaxis, motility, and transport/binding proteins were largely repressed under conditions of 24-h chromate treatment.

The metal oxyanion chromate (CrO_4^{2-}) is a widespread environmental contaminant due to its prevalent use in industrial and defense applications such as tanning, electroplating, paint pigment manufacturing, stainless steel welding, and nuclear weapons production (25, 26). The hexavalent form of chromium, Cr(VI), is highly soluble and toxic, with chronic exposure leading to mutagenesis and carcinogenesis. Cr(VI)-induced apoptosis, for example, was demonstrated in p53 human bronchoalveolar cells (46), and Cr(VI) exposure results in a spectrum of genomic damage in cultured cells including DNA single-strand and double-strand breaks, binding of amino acids and proteins to DNA, DNA interstrand cross-links, and Cr-DNA adducts (11, 27, 28, 43, 47, 53, 59, 64, 65). Cr toxicity is also associated with the generation of reactive oxygen intermediates during the intracellular partial reduction of Cr(VI) to the unstable intermediate Cr(V) by various in vivo nonspecific reductants (e.g., glutathione, NADH, NADPH, and cysteine) or cellular one-electron reductases (16, 27, 50). The other most stable, common form of chromium, trivalent Cr(III), is considered less toxic than Cr(VI) because of its tendency to form insoluble hydrated Cr^{3+} complexes, which cannot cross cell membranes. However, Cr(III) was shown to cause DNA damage and inhibit topoisomerase DNA relaxation activity in bacteria (40).

The adverse biological impact of Cr(VI) is attributable to the cellular uptake process. Chromate is transported across eukaryotic and prokaryotic cellular membranes via surface anion transport systems, namely, the sulfate transport system (16, 36, 38). Microorganisms have evolved diverse resistance mechanisms to cope with chromate toxicity. These detoxification strategies include biosorption, diminished intracellular accumulation through either direct obstruction of the ion uptake system or active chromate efflux, precipitation, and reduction of Cr(VI) to the less toxic, less mobile Cr(III) (reviewed in reference 16). Plasmid-determined resistance to chromate, for example, has been shown to occur in bacteria, including species of *Pseudomonas* (9, 17, 49) and *Alcaligenes* (36). A hydrophobic protein with 12 proposed transmembrane-spanning domains, designated ChrA, was found to be responsible for the plasmid-specified resistance phenotype in these organisms (16, 18, 37) and appears to function as a secondary transport system for the extrusion of chromium ions (3).

The in situ microbial catalysis of Cr(VI) reduction to sparingly soluble, less bioavailable Cr(III) has been proposed as a potential remediation strategy for Cr(VI)-contaminated subsurface environments. *Shewanella oneidensis* MR-1, a facultatively anaerobic γ-proteobacterium, possesses diverse metal-reducing capabilities, including the ability to transform Cr(VI) to Cr(III) (34, 56). As a result, its potential utility in the

* Corresponding author. Mailing address: Department of Biological Sciences, Purdue University, 1-118 Lilly Hall of Life Sciences, 915 West State Street, West Lafayette, IN 47907-2054. Phone: (765) 496-8301. Fax: (765) 494-0876. E-mail: dthomps@purdue.edu.

bioremediation of dissolved metal ions prompted the complete sequencing of the *S. oneidensis* MR-1 genome (23). Predicting the utility of *S. oneidensis* MR-1 for remediating metal-contaminated sites requires an understanding of the gene/protein components and cellular pathways enabling heavy metal resistance and biotransformation. In addition, the efficacy of in situ chromate bioremediation will depend on the capacity of remediating bacteria to cope with and perhaps minimize the cellular effects of heavy metal toxicity. Knowledge of the molecular and physiological response of MR-1 to Cr(VI) toxicity, in particular prolonged or chronic exposures, remains limited, however.

The primary goal of this work was to gain insight into global changes in the mRNA and protein expression patterns that occur in *S. oneidensis* MR-1 cells at a time point (in this case, 24 h) marked by the complete removal of chromate from the culture medium. We refer to this prolonged exposure to Cr(VI) and its derivatives as a "chronic" challenge to distinguish it from acute exposures before the onset of Cr(VI) reduction. Both transcriptome profiling and whole-cell proteomic analysis revealed that the predominant molecular response to chronic chromate exposure in complex medium was the induction of prophage-related genes and their encoded products as well as a number of functionally undefined hypothetical genes clustered within the lambda- and mu-like integrated phage regions of the MR-1 genome. In addition, a number of genes and/or their corresponding proteins with annotated functions in DNA metabolism (*topB*, *hsdM-2*, *uvrD*, and *recO*), electron transport (NADH dehydrogenase gene cluster, SO3056, and SO4360), cell division (*era*, *ftsAZ*, and *ftsL*), biosynthesis of murein (peptidoglycan) sacculus (*rodA*, *mreD*, *murE*, *murF*, *murG*, and *mraY*), and protein fate and general environmental stress responses (*htpG*, SO3391, *hslVU*, *ibpA*, *groES*, and *groEL*) were induced, while genes encoding regulatory, chemotaxis, motility, and transport/binding proteins were generally repressed. The accompanying physiological response to chronic Cr(VI) exposure included marked changes in cellular morphology as revealed by scanning confocal microscopy and atomic force microscopy (AFM). This study combines cell imaging, transcriptional measurement, and proteomic characterization to provide insight into the response and susceptibility of *S. oneidensis* MR-1 to 24-h chromate exposure.

MATERIALS AND METHODS

Bacterial strains, growth conditions, and assays. The *S. oneidensis* wild-type strain MR-1 (35) was cultivated aerobically at 30°C in Luria-Bertani (LB) medium (pH 7.2) or in LB medium amended with 0.3 mM potassium chromate (K_2CrO_4; Sigma-Aldrich Co., St. Louis, MO) with shaking at 250 rpm in a New Brunswick Scientific (Edison, NJ) incubator. A starter culture was prepared by inoculating LB medium amended with 0.3 mM chromate with a single colony of *S. oneidensis* MR-1 from a freshly streaked LB plate and allowing the cells to grow in the presence of chromate for 24 h. An aliquot of this starter culture, giving an initial optical density at 600 nm (OD_{600}) of 0.08, was used to inoculate fresh LB medium containing either 0 or 0.3 mM potassium chromate. OD_{600} was monitored in triplicate using either a Spectronic 20D+ spectrophotometer (Thermo Electron Cooperation, Waltham, MA) or the Bioscreen C microbiological culture system (Growth Curves USA, Piscataway, NJ) as described elsewhere (13). SigmaPlot version 8.0 (SPSS Inc., Chicago, IL) was used to plot growth curves.

Extracellular Cr(VI) was quantified spectrophotometrically at a wavelength of 540 nm using the 1,5-diphenylcarbazide (DPC) method as described elsewhere (39). Cultures were assayed at different time points (0, 3, 6, 9, 12, 15, 18, 21, and 24 h) during growth to determine the amount of residual Cr(VI) remaining in the

medium by measuring absorbance at 540 nm using a Varian (Cary-1E) UV-visible spectrophotometer (Hewlett-Packard, Wilmington, DE). Uninoculated LB medium containing 0.3 mM chromate served as the abiotic control.

Confocal laser scanning microscopy. *S. oneidensis* MR-1 cells were grown aerobically for 24 h in LB medium in the presence or absence of 0.3 mM chromate. Cells were then harvested and stained using the LIVE/DEAD *Bac*Light bacterial viability kit (Molecular Probes, Eugene, OR) in accordance with the manufacturer's instructions. Following a wash in distilled water, cells were filtered onto Isopore membrane filters (Millipore Corporation, Bedford, MA). The stained cells were viewed by confocal laser scanning microscopy using a TCS SP2 microscope (Leica Microsystems, Inc., Exton, PA). Z-series optical sections of cells were taken at 0.5 μm spacing and processed using Leica confocal software.

AFM. Following 24-h exposure in LB medium alone (control sample) or LB medium containing 0.3 mM chromate (experimental sample), MR-1 cells were fixed in 4% paraformaldehyde for 16 to 18 h at ambient temperature. After fixation, cells were pelleted by centrifugation at 3,000 rpm for 3 min and then resuspended in distilled water. A drop of the resuspended cells was placed on a polylysine-coated microscope slide and left undisturbed for 15 min. Slides were washed briefly with distilled water, dried, and mounted for imaging. AFM images were recorded using a PicoPlus atomic force microscope (Molecular Imaging Inc., Tempe, AZ) with a 100-μm scanning head. The instrument was operated in MacMode using silicon cantilevers (type II Maclevers; Molecular Imaging, Tempe, AZ) with a spring constant of 2.8 N/m at a scan speed of 0.8 lines/second at 512 pixels per line scan. All of the images presented are first order flattened.

RNA isolation, microarray hybridization, and data analysis. For transcriptome characterization, a starter culture, which was preexposed to 0.3 mM chromate for 24 h, was used to inoculate 100 ml of LB medium only (control samples) or LB medium containing 0.3 mM chromate (experimental samples) in 250-ml sidearm Pyrex flasks. A total of three separate control cultures and three separate experimental cultures were permitted to grow aerobically in parallel at 30°C for 24 h, at which time cells were harvested for total RNA extraction by centrifugation at maximum speed in a 5415R centrifuge (Eppendorf, Westbury, N.Y.) for 30 s at 4°C and washed once in ice-cold LB medium to remove residual chromate. RNA isolation, fluorescein-labeled cDNA preparation, and probe purification were carried out essentially as described previously (13).

An *S. oneidensis* MR-1 whole-genome open reading frame array containing approximately 95% of the total predicted MR-1 gene content was used to examine the global transcriptional response to 24-h chromate exposure. Construction of this array has been described previously (13, 20). Global gene expression profiling was performed using six independent microarray experiments (three biological replicates and two dye reversal reactions) as described in our previous study (14). Microarray prehybridization, hybridization, and posthybridization washings were carried out as described previously (13). The arrays were scanned as described elsewhere (52). Image quantification, data normalization, and analysis of gene expression data for statistical significance have been described previously (13). Transcripts exhibiting a statistically significant change in expression ($P < 0.05$) and a twofold or greater change in magnitude were considered for further analysis (48). The complete microarray data set for this study is available as supplemental Table S1 and can be accessed online (http://compbio.ornl.gov/shewanella_metal_stress/chronic).

RT-qPCR analysis. Reverse transcriptase, quantitative real-time PCR (RT-qPCR) was used to provide an independent assessment of gene expression for selected MR-1 genes. Six selected genes (SO0404, SO2426, SO2823, SO2945, SO3056, and SO3585) found to be differentially expressed by microarray hybridization were examined by comparative RT-qPCR as described elsewhere (13, 61). These genes are predicted to encode two hypothetical proteins (SO0404 and SO2945), two signal transduction response regulators (SO2426 and SO2823), a tetraheme cytochrome *c* (SO3056), and a putative azoreductase (SO3585). Relative expression patterns for each selected gene were independently confirmed using the following primer pairs, which were designed using the program Primer3 (http://www-genome.wi.mit.edu/cgi-bin/primer/primer3_www.cgi): SO0404, 5′-AGTATAACCAAGCGCCAGTA and 3′-GCATCG GTATTAACTTGCTC; SO2426, 5′-GCAGAAGGATTTAGGTCGAT and 3′-GCCACAACTAATTTCATGCG; SO2823, 5′-CGACACCTTACCTAAA ATCG and 3′-GGCATCTATGGGTTTGAGTA; SO2945, 5′-CTGACTTGC GGGATAAATAC and 3′-GGTAAGTGACGAACATCCAT; SO3056, 5′-G ATGCAGTAGTTGTCATGGA and 3′-CAGACTATCGTGGGGATTAG; SO3585, 5′-CGAGGCTATCCATCACTTAG and 3′-TGGAAAACACGAT AAAGACC.

Reagents and proteome preparation for liquid chromatography-tandem mass spectrometry (LC-MS/MS) analysis. All chemical reagents were obtained from Sigma Chemical Co. (St. Louis, MO) unless stated otherwise. Modified sequenc-
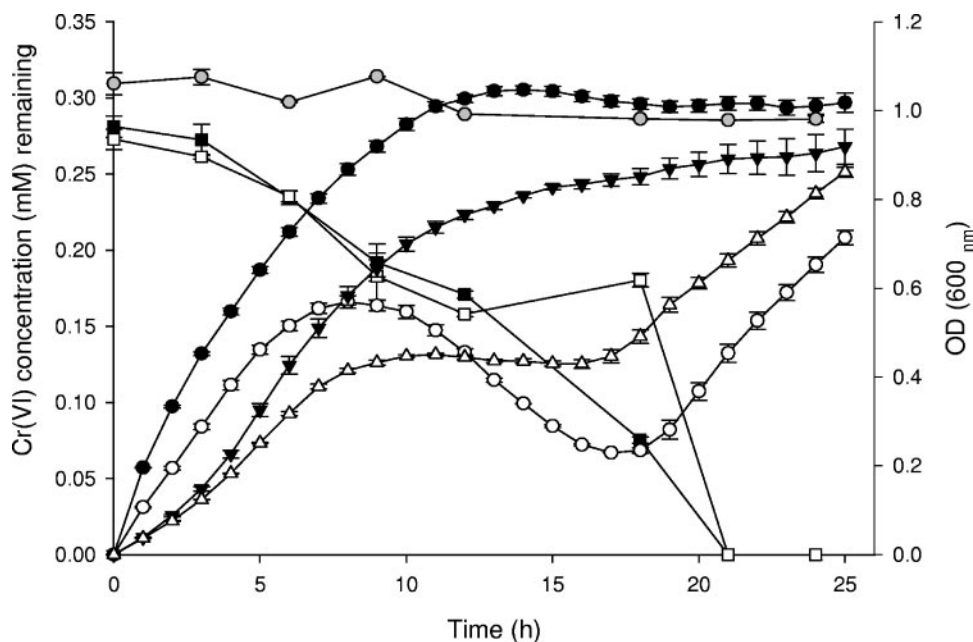
FIG. 1. Optical density and Cr(VI) disappearance patterns for *S. oneidensis* MR-1. Initially, cells were grown in LB medium containing 0.3 mM potassium chromate (preexposed) or LB medium only for 24 h under aerobic growth conditions at 30°C. An aliquot of the initial preexposed culture was then used to inoculate fresh LB medium only (▼) or LB medium containing 0.3 mM chromate (Δ), while the culture that was not preexposed to Cr(VI) was used to inoculate LB medium only (●) or LB medium containing 0.3 mM chromate (○). Culture density was monitored for 24 h under aerobic conditions using a Bioscreen C reader, and measurements represent mean OD_{600} ± standard errors (bars) for three replicate determinations. Residual Cr(VI) in the medium was quantified spectrophotometrically in parallel for cells exposed to 0.3 mM chromate (preexposed [■] and not preexposed [□]) over time using the DPC assay as described in reference 39. Uninoculated LB medium containing 0.3 mM chromate served as the negative control (gray circles). Graphed values represent the mean concentrations ± standard errors (bars) of three independent measurements performed in triplicate.

ing grade trypsin (Promega, Madison, WI) was used for all digestions. High-pressure LC (HPLC) grade water and acetonitrile (ACN) were acquired from Burdick & Jackson (Muskegon, MI), and 99% formic acid was purchased from EM Science (Darmstadt, Germany).

S. oneidensis MR-1 cells analyzed by mass spectrometry were cultivated as described above for the transcriptome characterization. Following 24-h growth in the absence or presence of 0.3 mM chromate, *S. oneidensis* cells were lysed using the method described by Brown et al. (14). Samples were separated into crude and membrane protein fractions using high-speed ultracentrifugation (100,000 × *g* for 60 min at 4°C) and were quantified using bicinchoninic acid analysis (Pierce, Rockford, IL). Approximately 2 mg of protein from each proteome fraction for the two different growth conditions was digested with sequencing grade trypsin at 1:100 (wt/wt) as described previously (14). Samples were immediately desalted using Sep-Pak Plus C_{18} solid-phase extraction (Waters, Milford, MA). Using a Savant SpeedVac (Thermo Electron Corporation, Waltham, MA), samples were concentrated and solvent exchanged into 0.1% formic acid in water to ~10 μg/μl starting material and then filtered, aliquoted, and frozen at −80°C until ready for LC-MS/MS analysis.

LC-MS/MS analysis. The experimental (treated with chromate for 24 h) and control (untreated) proteome samples were analyzed in duplicate via two-dimensional (2-D) LC-MS/MS analysis with an Ultimate HPLC (LC Packings, a division of Dionex, San Francisco, CA) connected to an LTQ linear trapping quadrupole (Thermo Finnigan, San Jose, CA). The HPLC pump was set at a flow rate of ~100 μl/min, which was split precolumn to achieve a final flow rate of ~200 nl/min at the nanospray tip. A split-phase column was packed as described previously (14) with approximately 500 μg of each sample loaded onto the column via a pressure cell. This loaded column was then placed behind a PicoFrit tip (inner diameter [I.D.], 100 μm; 15-μm I.D. at the tip; New Objective, Woburn, MA) packed in-house via a pressure cell with ~15 cm of the reverse phase (Aqua C_{18} 5-μm 200A Phenomenex). The columns were positioned in front of the LTQ on a nanospray source (Thermo Finnigan).
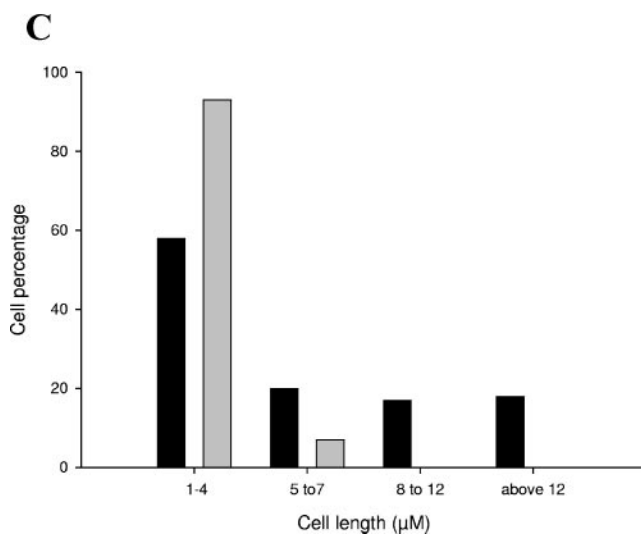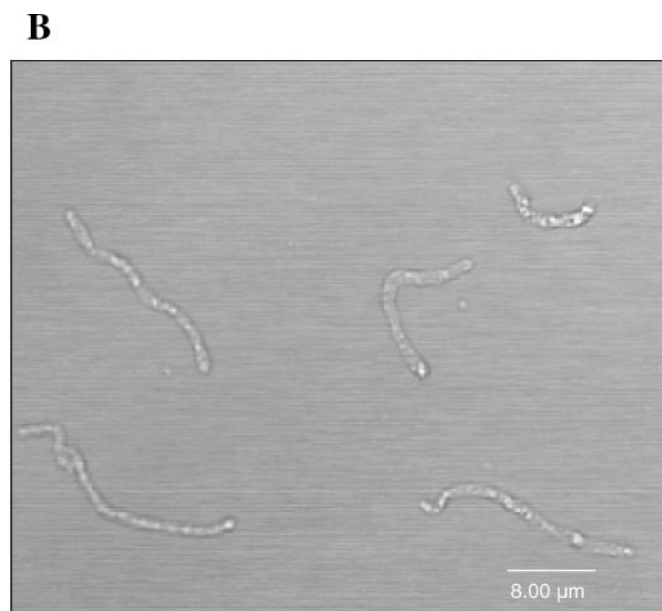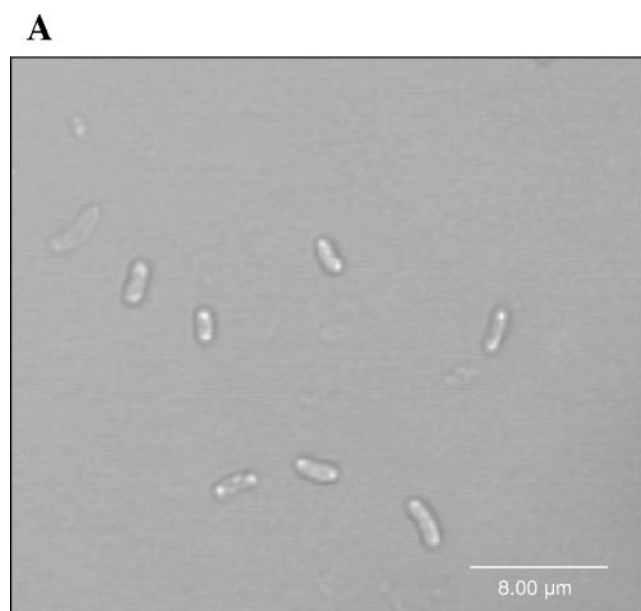
All control and experimental samples were subjected to a 24-h 12-step 2-D analysis with an increasing amount (0 to 500 mM) of ammonium acetate via salt pulses accompanied by a 2-h 100% aqueous solvent (95% H₂O–5% ACN–0.1%

formic acid)-to-50% organic solvent (30% H₂O–70% ACN–0.1% formic acid) gradient (method adapted from reference 29). The LTQ was run in the data-dependent MS/MS mode during the entire chromatographic procedure. Chromatographic methods and HPLC columns were identical for all sample analyses. The LC-MS/MS system was fully automated and under direct control of the Xcalibur software system (Thermo Finnigan).

Proteome bioinformatics. The *S. oneidensis* MR-1 protein database used in MS/MS spectrum searches consisted of the latest genome annotation (http://www.tigr.org/) along with 36 common contaminating proteins (e.g., trypsin and keratin from the sample preparation procedure); the database is available for download at the project website http://compbio.ornl.gov/shewanella_metal_stress/chronic/databases/. MS/MS spectra were searched against the MR-1 database using SEQUEST (Thermo Electron) with cross-correlation scores of at least 1.8 (+1), 2.5 (+2), and 3.5 (+3), as described previously (14). Output data files were filtered at the one- and two-peptide levels, sorted, and compared as detailed by Brown et al. (14). Supplemental Table S2 (available online at http://compbio.ornl.gov/shewanella_metal_stress/chronic/supplemental) contains a list of all proteins identified at the two-peptide level organized according to the percentage of the protein sequence identified (percent sequence coverage), the number of peptides identified for the protein (peptide count), and the number of spectra that were confidently identified for the proteins (spectral count). Differentially expressed proteins under chromate conditions were identified using a semiquantitation method based on the following criteria: greater-than-40% sequence coverage, five or more unique peptides, and/or a twofold difference in the number of mass spectra identified under the control conditions versus the experimental conditions (14, 55, 61).

RESULTS AND DISCUSSION

Effects of prolonged chromate exposure on MR-1 growth and morphology. Our previous work investigating the molecular response of *S. oneidensis* MR-1 to an acute chromate

A

B

C

FIG. 2. Morphological characterization of *S. oneidensis* MR-1. Shown are scanning confocal micrographs of cultures of wild-type *S. oneidensis* grown aerobically for 24 h in (A) complex LB medium or (B) LB medium containing an initial chromate concentration of 0.3 mM. Unstained cells were imaged in bright-field mode using a Leica TCS SP2 scanning confocal microscope. (C) Frequency distribution of *S. oneidensis* cell lengths for untreated control cells (gray bars) and cells exposed to Cr(VI) for 24 h (black bars). Cells were stained using the *Bac*Light bacterial viability kit and imaged using a Leica TCS SP2 scanning confocal microscope. Randomly selected cells (100 cells per treatment) were measured and sorted into groups according to their sizes. Measurements were made using the Leica confocal software.

challenge (a maximum exposure time of 90 min) indicated a MIC of chromate (K_2CrO_4) of approximately 2 mM under aerobic conditions in LB medium (14). Growth studies were conducted to determine whether preexposure to a sublethal dose of chromate, in this case 0.3 mM, increased cellular tolerance to this heavy metal. Preexposed cells attained a slightly higher OD_{600} at the 24-h time point compared to cells that had not been preexposed to Cr(VI) (Fig. 1). Similar to our previous observations (14), cells exhibited a biphasic OD pattern in the presence of 0.3 mM Cr(VI), regardless of whether cells had been preexposed (Fig. 1). Cr(VI) disappearance continued to occur during periods where the OD of chromate-treated cultures either changed very little (resembling a stationary-phase plateau) or actually declined, while the second phase of OD increase (at ~18 h) coincided with the appearance of cells displaying extremely elongated or filamentous morphology (data not shown for the 18-h time point). Hence, the increases

in OD_{600} observed after about 18 h may not be an accurate reflection of cell growth but may be due largely to the drastic changes in cell size. This was shown to be the case for *Escherichia coli* K-12 cells, which also exhibited biphasic growth kinetics in chromate-amended LB medium (2).

The impact of Cr(VI) exposure on the cell morphology and surface topology of *S. oneidensis* cells was examined by confocal laser scanning microscopy and AFM. The results indicated that cells from 24-h cultures with no detectable extracellular Cr(VI) formed long, apparently aseptate filaments in contrast to the normal rod-shaped morphology exhibited by untreated cells (Fig. 2). As shown in Fig. 2C, the majority (approximately 93%) of examined control cells (grown in LB medium only) appeared normal in size (~1 to 4 μm in length) and were motile, while only a small percentage (7%) fell within the size range of 5 to 7 μm. However, only about 58% of the cells subjected to 24-h chromate exposure had sizes within the nor-
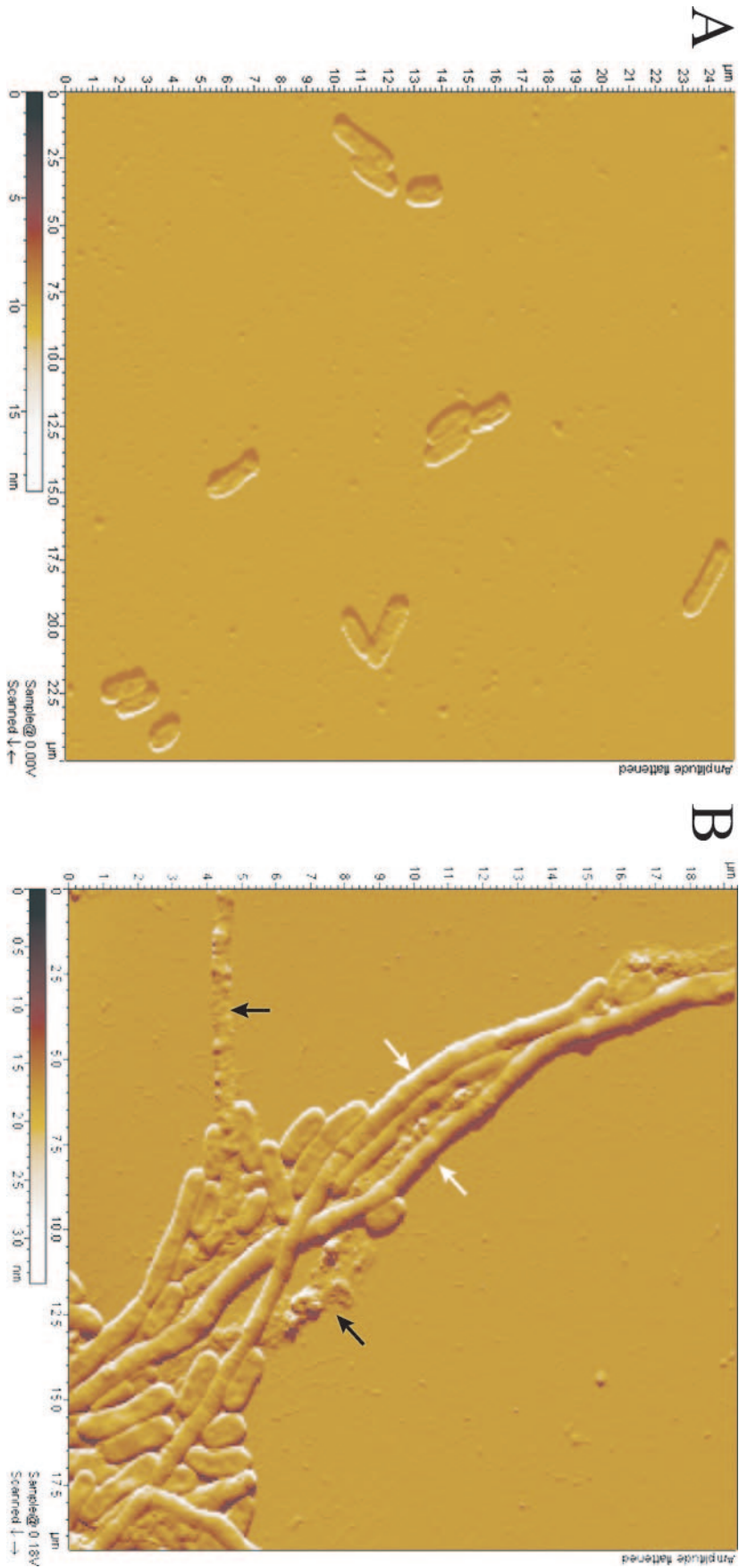
FIG. 3. AFM images of *S. oneidensis* exposed for 24 h in (A) LB medium or (B) LB medium containing an initial chromate concentration of 0.3 mM. Cells were fixed in 4% paraformaldehyde, mounted on poly-L-lysine-coated microscope slides, and air dried prior to imaging. Images were recorded using a PicoPlus atomic force microscope. White arrows denote elongated intact cells; black arrows indicate the apparent breakdown of the cell membrane and lysis.

TABLE 1. Functional distribution of the observed and predicted MR-1 proteomes

Functional category (no.)	No. of proteins		%[c]	No. of proteins[d]	
	Observed[a]	Predicted[b]		Upregulated	Downregulated
Amino acid biosynthesis (1)	72	91	79.1	4	0
Biosynthesis of cofactors, prosthetic groups, and carriers (2)	95	121	78.5	0	1
Cell envelope (3)	115	180	63.9	3	5
Cellular processes (4)	175	260	67.3	0	7
Central intermediary metabolism (5)	28	51	54.9	3	0
DNA metabolism (6)	84	144	58.3	5	0
Energy metabolism (7)	205	308	66.6	1	5
Fatty acid and phospholipid metabolism (8)	45	65	69.2	0	0
Hypothetical proteins (9)	633	2,039	31.0	20	20
Mobile and extrachromosomal element functions (10)	45	317	14.2	14	0
Protein fate (11)	131	185	70.8	2	4
Protein synthesis (12)	128	141	90.8	0	1
Purines, pyrimidines, nucleosides, and nucleotides (13)	58	62	93.5	1	1
Regulatory functions (14)	104	199	52.3	0	2
Signal transduction (15)	34	61	55.7	0	0
Transcription (16)	45	54	83.3	0	0
Transport and binding proteins (17)	126	274	46.0	0	5
Unknown function (18)	190	379	50.1	3	2
Total	2,313	4,931	46.9	56	53

[a] Total number of proteins identified in this study with at least two peptides per protein from replicate analyses.
[b] Total number of predicted proteins based on annotation of the MR-1 genome (www.tigr.org).
[c] Percentage of the predicted proteome detected in this study.
[d] Number of proteins displaying increased (upregulated) or decreased (downregulated) abundance under Cr(VI) treatment based on sequence coverage as well as peptide and spectral counts.

mal range (i.e., ~1 to 4 μm in length), while 35% were ~8 μm or longer (in some cases ~25 μm) (Fig. 2C). Cells that were longer than normal were also nonmotile, and some appeared as aggregated filaments. These filamentous cells, in which septation was apparently impeded, were observed under conditions of complete Cr(VI) disappearance in the growth medium as indicated by the colorimetric DPC assay and not under acute chromate stress conditions characterized by short exposure times (e.g., 90 min) and no detectable Cr(VI) transformation (results not shown). This marked effect of chromate on cell morphology has been observed for other bacteria. Non-adapted *E. coli* K-12 cells exposed to 250 μM potassium chromate (K_2CrO_4) exhibited extreme filamentous morphology within 3 h of Cr(VI) challenge (2). An enlarged or elongated cell size also has been observed following exposure to other stress conditions, such as high salt (57), low-temperature growth at 3°C (1), and UV radiation (42), and likely constitutes a general cellular response to environmental stress. The increased cell size of *Staphylococcus aureus* under high NaCl was correlated with shorter interpeptide bridges, less cross-linked peptidoglycan, and retarded cell separation (57).

Consistent with the bright-field imaging results, *S. oneidensis* filamentation (Fig. 3B) was observed using AFM following a 24-h exposure to 0.3 mM chromate, which contrasted with the normal rod-shaped morphologies of untreated control cells. In some cases, damage to the cell surface was severe enough to lead to the apparent disintegration of the outer membrane and hence lysis of the bacterium (Fig. 3B), revealing the underlying cytoplasmic contents. AFM indicated a similar breach in the cell membrane integrity of *Escherichia coli* cells subjected to different concentrations of the β-lactam antibiotic cefodizime (10).

Transcriptome and proteome characterization of the *S. oneidensis* MR-1 response to 24-h Cr(VI) challenge. Microarray profiling and 2-D LC-MS/MS were performed to analyze the transcriptome and proteome, respectively, of *S. oneidensis* MR-1 at the 24-h time point following initial exposure to 0.3 mM chromate. Gene and protein expression profiles of cells exposed to chromate were compared to those of untreated control cells grown in parallel (see Materials and Methods for experimental details). Approximately 26% ($n = 1,215$) of the total predicted *S. oneidensis* MR-1 genes ($n = 4,648$) with representative probes on the array displayed at least a twofold statistically significant ($P < 0.05$) change in transcript expression at the 24-h time point following chromate exposure. RT-qPCR was used to provide an independent assessment of mRNA expression for targeted genes analyzed in the transcriptome experiment. The six genes (changes [n-fold] given in parentheses) selected for RT-qPCR analysis exhibited either upregulated or downregulated expression patterns as identified by microarray hybridization: SO0404 (14.4), SO2426 (0.45), SO2823 (13.4), SO2945 (271), SO3056 (8.5), and SO3585 (0.7). Comparison of gene expression measurements determined by RT-qPCR and microarray analysis indicated that the two different data sets were highly correlated, with a Pearson correlation coefficient, r, of 0.95.

At the protein level, a total of 2,313 gene products, representing 47% of the predicted MR-1 proteome, were identified at the two-peptide level in duplicate analyses of control samples and samples exposed to chromate for 24 h (Table 1). A total of 3,051 proteins were identified using the less stringent one-peptide filter level; however, a one-peptide filter level for the identification of proteins results in a dramatically higher false-positive discovery rate (44), so a thorough

analysis of only the two-peptide data is presented here. The levels of reproducibility between replicate analyses of the control proteome and the experimental (chromate-treated) proteome on the LTQ instrument were 75.6% and 77.2%, respectively. For the observed proteome identified in this study, 109 protein species were found to be differentially expressed under prolonged Cr(VI) exposure, with 56 proteins displaying increased abundance and 53 showing decreased abundance (Table 1). Supplementary transcriptome and proteome data (i.e., a list of all significantly expressed genes, the complete raw and filtered proteome data, and a list of differentially expressed proteins) can be accessed online at http://compbio.ornl.gov/shewanella_metal_stress /chronic/.

Proteins identified at the two-peptide level under the two different growth conditions were organized in Table 1 according to the functional categories assigned by The Institute for Genomic Research (see www.tigr.org; Comprehensive Microbial Resource). Using multidimensional HPLC-MS/MS, we identified more than 75% of the predicted MR-1 proteins for the following five functional categories: amino acid biosynthesis; biosynthesis of cofactors, prosthetic groups, and carriers; protein synthesis; purines, pyrimidines, nucleosides, and nucleotides; and transcription. Under 24-h Cr(VI) exposure, more proteins were identified in the functional categories of amino acid biosynthesis; biosynthesis of cofactors, prosthetic groups, and carriers; purines, pyrimidines, nucleosides, and nucleotides; and protein synthesis than were found under the corresponding control condition (Table 1).

Induction of prophage-related genes and proteins. Sequence analysis of the MR-1 genome revealed the presence of an integrated lambda-like phage (LambdaSo; 51,857 bp) and two phylogenetically distinct phages related to the *E. coli* mu (MuSo1 [34,551 bp] and MuSo2 [35,666 bp]) (23). The lambda-like phage genome is also present in MR-1 in a nonintegrated form (23). There are 75, 42, and 53 open reading frames (ORFs) annotated as LambdaSo, MuSo1, and MuSo2 genes, respectively (23).

A previous study focusing on *S. oneidensis* MR-1 demonstrated the induction of a large number of prophage-related genes in response to UV radiation, particularly those genes from the integrated LambdaSo genome, and the presence of phage particles in UV-irradiated MR-1 cultures (42). Based on transcriptome analysis, the genomic response of MR-1 to ionizing radiation (40 Gy) was found to be very similar to its response to UV radiation (41). Similarly, we observed the strong induction of numerous prophage-related genes in MR-1 cells exposed to chromate for 24 h (see supplemental Table S1 at http://compbio.ornl.gov/shewanella_metal_stress/chronic /supplemental; Table 2), suggesting that prolonged Cr(VI) exposure and/or the accumulation of intracellular chromium may induce the lytic cycle of lysogenic bacteriophage in MR-1. Overall, 16 (21%), 2 (5%), and 10 (19%) ORFs annotated as LambdaSo, MuSo1, and MuSo2 genes, respectively, were significantly induced (more than twofold; $P < 0.05$) in response to prolonged Cr(VI) exposure. This molecular response was in striking contrast to the differentially expressed genes/proteins characterizing the cellular response to a 90-min acute 1 mM chromate challenge, during which a very small subset of pre-

dicted prophage genes (i.e., six) displayed a moderate two- to fourfold induction (14).

Gene products for 14 ORFs with annotations corresponding to mobile and extrachromosomal element functions were confidently identified as being upregulated in response to prolonged Cr(VI) treatment based on both microarray analysis and multidimensional HPLC-MS/MS (Table 2). Ten of these 14 proteins were encoded in the LambdaSo genome, whereas 1 and 2 gene products were annotated as prophage MuSo1 and MuSo2 proteins, respectively. The majority of these genes encoded such prophage structural proteins as minor and major tail proteins, tail assembly components, and the major head subunit (Table 2). Six additional ORFs (SO2941, SO2969, SO2973, SO2978, SO2985, and SO3006) with prophage LambdaSo-related functions displayed significant increases (more than twofold; $P < 0.05$) in mRNA expression (see supplemental Table S1 at http://compbio .ornl.gov/shewanella_metal_stress/chronic/supplemental). The corresponding proteins for those genes were detected only under Cr(VI) conditions by HPLC-MS/MS analysis but failed to meet our filtering criteria for determining differential expression (see Materials and Methods and supplemental Table S2): SO2941 (~20% sequence coverage), SO2969 (protein not detected), SO2973 (~8.2%), SO2978 (~20%), SO2985 (~15%), and SO3006 (~15%). The genes encoded a putative LambdaSo-associated lysozyme (SO2973, 1,053.6-fold), tail assembly protein I (SO2941; 366.5-fold), a putative holin (SO2969, 49.2-fold), a site-specific recombinase (SO2978; 23.8-fold), replication protein O (SO2985, 4.4-fold), and a type II DNA modification methyltransferase (SO3006, 3.8-fold). Other upregulated prophage-related genes had predicted functions in virion morphogenesis (SO2690, 65.6-fold), DNA transposition (SO0644, 11.9-fold; SO2655, 3.6-fold) and circulation (SO2698, 4.1-fold), positive regulation of late transcription (SO2668, 16.7-fold), baseplate (SO2700, 4.3-fold) and tail assembly (SO2699, 10.3-fold; SO2704, 17.2-fold), and assembly of the major head subunit (SO0675, 5.9-fold; SO2685, 24.5-fold), as well as assembly of other structural components (SO2681, 6.2-fold; SO2684, 6.8-fold) (see supplemental Table S1).

Of the differentially expressed proteins determined as having increased abundance under Cr(VI) conditions, 36% corresponded to hypothetical or conserved hypothetical proteins (Table 2). Five of these proteins (SO2660, SO2663, SO2667, SO2673, and SO2688) are encoded by genes from the MuSo2 genome, which implied their potential function in prophage activation and synthesis. The majority of the upregulated hypothetical proteins (i.e., SO2942, SO2944 to -46, SO2950, SO2951, SO2955, SO2979, SO2980, SO2982, SO2988, SO3001, and SO3008) were derived from genes located in the LambdaSo genome, while no potentially MuSo1-related hypothetical or conserved hypothetical proteins were measured as being differentially expressed under our experimental conditions (Table 2). Transcriptome analysis revealed a considerably greater number of upregulated hypothetical and conserved hypothetical genes clustered within the three different prophage regions (see supplemental Table S1 at http://compbio.ornl.gov/shewanella_metal_stress/chronic /supplemental). Of the 258 induced hypothetical and conserved hypothetical genes observed, 86 (33%) were distributed among the prophage genomes of MuSo1 (12 genes), MuSo2 (30 genes), and LambdaSo (44 genes).

The gene and protein expression data strongly suggest that,

TABLE 2. Relative expression of upregulated proteins and their corresponding mRNA levels in response to 24-h chromate exposure

Gene	Gene product (functional category no.[e])	Transcriptomics [Cr(VI)/Con ratio][a]	Proteomics					
			Control			24-h chromate exposure		
			% Coverage[b]	No. of unique peptides/ protein[c]	Avg no. of spectra[d]	% Coverage	No. of unique peptides/ protein	Avg no. of spectra
SO0401	Alcohol dehydrogenase, zinc containing (7)	1.2	0.0	0	0	45.1	9	11
SO0644	Prophage MuSo1 DNA transposition protein (10)	11.9	0.0	0	0	72.4	15	25
SO0795	Conserved hypothetical protein (9)	0.80	5.9	2	1	49.7	16	16.5
SO2654	Putative transposase (10)	1.5	0.0	0	0	36.9	19	16
SO2655	Prophage MuSo2 DNA transposition protein (10)	3.6	16.0	3	2	57.5	18	57.5
SO2660	Conserved hypothetical protein (9)	14.1	32.5	5	6	83.5	24	145
SO2663	Conserved hypothetical protein (9)	8.5	0.0	0	0	58.7	12	36
SO2667	Conserved hypothetical protein (9)	19.7	0.0	0	0	48.0	8	10
SO2673	Hypothetical protein (9)	10.8	0.0	0	0	55.4	8	7.5
SO2685	Putative prophage MuSo2 major head subunit (10)	24.5	22.7	3	2	51.8	12	17.5
SO2688	Hypothetical protein (9)	24.5	0.0	0	0	42.0	10	6.5
SO2834	Anaerobic ribonucleoside-triphosphate reductase, NrdD (13)	1.9	16.6	8	8	37.2	20	30
SO2940	Prophage LambdaSo host specificity protein J (10)	5.4	3.7	2	1	49.6	49	107
SO2942	Hypothetical protein (9)	42.4	0.0	0	0	59.6	11	19
SO2944	Hypothetical protein (9)	44.7	0.0	0	0	65.3	26	96.5
SO2945	Hypothetical protein (9)	129.8	26.6	4	6.5	67.8	15	78
SO2946	Hypothetical protein (9)	37.2	0.0	0	0	58.0	10	65.5
SO2948	Prophage LambdaSo tail assembly protein K (10)	23.7	0.0	0	0	51.9	8	7.5
SO2949	Prophage LambdaSo minor tail protein L (10)	5.6	0.0	0	0	50.6	10	23.5
SO2950	Hypothetical protein (9)	10.9	0.0	0	0	53.4	9	23.5
SO2951	Hypothetical protein (9)	48.5	16.9	5	4	69.2	41	172.5
SO2952	Prophage LambdaSo minor tail protein M (10)	28.6	0.0	0	0	82.0	6	14.5
SO2953	Prophage LambdaSo tail length tape measure protein H (10)	33.4	4.2	2	2	58.5	51	74
SO2955	Conserved hypothetical protein (9)	74.9	14.0	1	1.5	46.3	7	20
SO2956	Prophage LambdaSo major tail protein V (10)	61.9	0.0	0	0	80.9	8	57.5
SO2963	Prophage LambdaSo major capsid protein, HK97 family (10)	168.0	36.6	12	13	80.8	32	183.5
SO2964	ClpP protease family protein (11)	57.7	0.0	0	0	23.6	7	11
SO2965	Prophage LambdaSo portal protein, HK97 family (10)	106.0	14.8	2	1	41.9	14	16
SO2979	Hypothetical protein (9)	11.7	0.0	0	0	45.0	7	8.5
SO2980	Hypothetical protein (9)	8.9	0.0	0	0	69.1	11	12.5
SO2982	Hypothetical protein (9)	8.2	0.0	0	0	49.7	7	8.5
SO2988	Conserved hypothetical protein (9)	4.2	69.2	7	6.5	95.3	23	84.5
SO2993	Putative prophage LambdaSo type II DNA modification methyltransferase (10)	3.3	0.0	0	0	67.2	19	42.5
SO3001	Hypothetical protein (9)	8.4	0.0	0	0	80.6	9	28
SO3004	Putative prophage LambdaSo DNA modification methyltransferase (10)	2.4	0.0	0	0	68.2	21	51.5
SO3008	Hypothetical protein (9)	2.0	0.0	0	0	56.2	6	10.5
SO3013	Site-specific recombinase, phage integrase family (6)	1.4	0.0	0	0	24.3	11	10.5
SO3019	Anthranilate synthase component I, TrpE (1)	1.3	5.9	2	1	45.6	19	32
SO3020	Glutamine amidotransferase, TrpG (1)	2.5	0.0	0	0	51.0	6	8.5
SO3022	Isomerase, TrpC/F (1)	1.6	13.0	5	2.5	45.2	19	33.5
SO3061	DNA topoisomerase III, TopB (6)	1.3	8.0	3	3	37.9	18	16
SO3183	Perosamine synthetase-related protein (18)	3.3	12.7	3	2.5	46.8	10	12.5
SO3185	Polysaccharide biosynthesis protein (3)	3.4	9.5	2	1	55.9	12	14.5
SO3189	Polysaccharide biosynthesis protein (3)	2.2	28.2	7	9	70.9	18	34.5
SO3315	Conserved hypothetical protein TIGR00048 (9)	0.80	0.0	0	0	36.5	10	9.5
SO3726	Sulfate adenylyltransferase, subunit I, CysN (5)	2.4	14.7	3	4	45.9	14	22.5
SO3727	Sulfate adenylyltransferase, subunit 2, CysD (5)	2.2	16.6	4	2.5	54.6	11	23.5
SO3737	Sulfite reductase (NADPH) hemoprotein beta component, CysI (5)	2.1	3.7	2	1	45.7	17	27
SO3797	Peptidase, U32 family (11)	1.0	0.0	0	0	28.1	10	10.5
SO4265	Type I restriction-modification system, M subunit, HsdM-2 (6)	1.1	22.9	6	6.5	52.9	17	20.5
SO4309	Diaminopimelate decarboxylase, LysA (1)	0.70	11.1	3	2	46.4	11	16.5
SO4343	Aminotransferase, class V (18)	1.7	0.0	0	0	59.3	14	24
SO4686	NAD-dependent epimerase/dehydratase family protein (3)	1.1	0.0	0	0	50.1	10	7
SOA0003	Putative type II restriction endonuclease (6)	0.70	16.7	3	1.5	50.9	17	23
SOA0004	Type II DNA modification methyltransferase (6)	0.90	13.0	4	4	54.9	24	44
SOA0160	Putative esterase (18)	0.70	30.5	6	7.5	63.4	11	21

[a] Relative gene expression (induction) is presented as the mean ratio of the fluorescence intensity of Cr(VI)-exposed cells (experimental) to control (nonexposed; Con) cells.
[b] Total sequence coverage from replicate analyses.
[c] Total number of unique peptides identified per protein from replicate analyses.
[d] Average number of spectra identified per protein from replicate analyses.
[e] From Table 1.

similar to UV irradiation (42), prolonged exposure to chromate and its derivatives may activate the lytic cycles of some or all three of the MR-1 prophages, leading to prophage-mediated cell lysis. At this point, it is not clear whether the induction of MR-1 prophage-related genes/structural proteins is a response to an extended Cr(VI) exposure per se or to the possible intracellular accumulation of chromium, particularly reduced Cr(III). *S. oneidensis* MR-1 cells exposed to Cr(VI) have been shown to precipitate reduced chromium both extracellularly on the cell surface and as electron-dense globules inside cells (30). Qiu et al. (42) suggested that prophage activation was the major lethal factor in *S. oneidensis* MR-1 following UV C or UV B irradiation. Our results certainly point to prophage activation as a major contributor to the toxic effects of Cr(VI) under conditions of prolonged exposure and reduction.

Cell wall biosynthesis and cell division gene cluster. Bacterial cell growth occurs by the coordinated periodic alternation of morphogenesis (elongation) and cell division events (19). Central to bacterial morphogenetic processes is biosynthesis and turnover of the peptidoglycan (murein) sacculus, which functions as the principal stress-bearing and shape maintenance component of the cell wall (reviewed in reference 60). The Mur ligases and MurG (a glycosyltransferase) are key enzymes in peptidoglycan biosynthesis and are essential for bacterial cell growth, while formation of the *E. coli* cell septum involves proteins encoded by *fts* (temperature-sensitive filamentation) genes (for reviews, see references 15 and 63). Hierarchical assembly of the divisome is initiated by localization of the FtsZ protein near the site of cell division and formation of a ring-like polymeric structure (8), followed by the sequential recruitment of the remaining cell division proteins to the septum site. Cells defective in the expression of FtsI, FtsL, and FtsQ give rise to abnormal morphologies characterized by long, aseptate filaments that eventually lyse (22).

An observation to emerge from the transcriptome study was the upregulation of seven ORFs within the cell wall biosynthesis and cell division gene cluster corresponding to the SO4214-SO4228 region on the MR-1 chromosome. This chromosomal region comprises 15 ORFs with the following gene order: SO4228, SO4227, *ftsL* (SO4226), *ftsI* (SO4225), *murE* (SO4224), *murF* (SO4223), *mraY* (SO4222), *murD* (SO4221), *ftsW* (SO4220), *murG* (SO4219), *murC* (SO4218), *ftsQ* (SO4217), *ftsA* (SO4216), *ftsZ* (SO4215), and *lpxC* (SO4214) (23) (www.tigr.org). These 15 *S. oneidensis* MR-1 genes are transcribed from the same DNA strand with very small, if any, intergenic regions, suggesting that the cluster may constitute a single operon. Seven of the 15 genes exhibited statistically significant ($P < 0.05$) but moderate increases in mRNA expression at the 24-h time point of Cr(VI) exposure: *ftsL* (2.9-fold), *murE* (3.4-fold), *murF* (2.0-fold), *mraY* (5.4-fold), *murG* (3.4-fold), *ftsA* (2.1-fold), and *ftsZ* (2.1-fold). The corresponding proteins for these genes were not identified as being upregulated by our shotgun proteomics methodology (see supplemental Table S2 at http://compbio.ornl.gov /shewanella_metal_stress/chronic/supplemental).

In addition to certain *fts* and *mur* genes, *S. oneidensis* ORFs coding for homologs of *E. coli* proteins implicated or known to function in determining the rod-like morphology of the cell (*rodA* and *mreD*), cell cycle regulation (*era*), and intracellular

septation (*ispZ*) were induced two- to threefold at the transcript level under our conditions of Cr(VI) exposure. Disruption of the *rodA* locus in *Streptococcus thermophilus* resulted in abnormal cell morphologies as well as an increased susceptibility of the mutant to oxidizing agents (e.g., hydrogen peroxide), indicating a possible role for RodA in oxidative stress defense (51). In addition, depleting the cellular concentration of Era or impairing its GTPase activity results in bacterial cell cycle arrest and causes elongation of *E. coli* cells (12, 21). Taken together, the abnormally elongated morphologies of *S. oneidensis* cells exposed to prolonged Cr(VI) treatment and upregulated transcript levels for a number of genes putatively involved in cell wall biosynthesis, septation, and morphogenesis might indicate interference with normal cell division by the accumulation of intracellular chromium species. However, more research is needed to substantiate this possible explanation.

Membrane response and general stress-associated genes. The magnitude of the stress imposed by heavy metals and an organism's resistance ability will necessarily intersect metal reduction processes. A recent transcriptome study of *S. oneidensis* MR-1 exposed to a diverse array of metal (Cr was not included) and nonmetal terminal electron acceptors pointed to the induction of detoxification and stress response genes as playing an important role in the adaptation of MR-1 under anoxic metal-reducing conditions (6). Other transcriptional-profiling investigations of *S. oneidensis* and *Caulobacter crescentus* also demonstrated the induction of oxidative stress protection genes in response to chromate treatment (7, 14, 24).

The sensitivity of *S. oneidensis* MR-1 correlated with the induction of stress-associated genes in response to 24-h Cr(VI) exposure. A number of molecular chaperones or environmental stress response genes were upregulated under our experimental conditions: *groES* (5.8-fold), *groEL* (5.8-fold), *htpG* (4.4-fold), *ibpA* (4.8-fold), and *hslU* (4.7-fold) (see supplemental Table S1 at http://compbio.ornl.gov /shewanella_metal_stress/chronic/supplemental). The proteins encoded by these genes mediate the correct folding of a fraction of de novo polypeptides and function in the reactivation or degradation of proteins damaged by different types of stressors. In addition, the gene encoding iron-dependent superoxide dismutase, *sodB*, was induced 2.3-fold under our experimental conditions. Other transcriptional changes included upregulation of genes coding for ATP-dependent proteases (SO3391, *hslV*) and a number of ribosomal proteins (SO0226, SO0227, SO0231 to SO0240, SO0243, SO0244, and SO0246 to SO0249).

The membrane response was characterized by changes in the expression of genes encoding outer membrane structural components and polysaccharide biosynthesis proteins. Induced genes included those encoding putative outer membrane porins (encoded by SO0312 and SO1821), OmpW (encoded by SO1673), and three proteins with functions related to polysaccharide biosynthesis (encoded by SO3158, SO3181, and SO3185). Proteomic analysis indicated increases in the synthesis of SO3185 and SO3189, both annotated as polysaccharide biosynthesis proteins, while four predicted lipoproteins (SO2570, NlpD, SOA0110, and SOA0112) and an OmpA family protein (SO3969) belonging to the functional category of cell envelope proteins showed decreased abundance under Cr(VI) condi-

TABLE 3. Relative expression of downregulated proteins and their corresponding mRNA levels in response to 24-h chromate exposure

Gene	Gene product (functional category no.[f])	Transcriptomics [Cr(VI)/Con ratio][a]	Proteomics					
			Control			24-h chromate exposure		
			% Coverage[b]	No. of unique peptides/protein[c]	Avg no. of spectra[d]	% Coverage	No. of unique peptides/protein	Avg no. of spectra
SO0433	Regulator of sigma D, Rsd (14)	0.70	67.7	12	19	36.0	5	2.5
SO0576	PhoH family protein (18)	0.80	58.6	19	22.5	0.0	0	0
SO0902	NADH:ubiquinone oxidoreductase, Na translocating, alpha subunit, NqrA-1 (7)	1.0	70.6	24	24	16.7	6	6
SO1144	Methyl-accepting chemotaxis protein (4)	0.60	86.5	33	71.5	31.8	9	12.5
SO1425	Hypothetical protein (9)	1.0	44.8	17	13	0.0	0	0
SO1518	Conserved hypothetical protein (9)	0.60	85.7	14	39	39.7	7	8
SO1689	Cation transport ATPase, E1-E2 family (4)	0.40	30.0	13	10	0.0	0	0
SO1700	Hypothetical protein (9)	0.90	61.2	21	23.5	0.0	0	0
SO2062	Conserved hypothetical protein (9)	0.50	63.8	12	29	44.0	3	5.5
SO2247	Hypothetical protein (9)	0.40	38.4	12	12	0.0	0	0
SO2304	Alanine dehydrogenase, authentic point mutation, Ald (7)	0.40	67.7	20	62.5	23.5	4	10
SO2469	Conserved hypothetical protein (9)	0.60	67.9	61	90.5	8.8	5	2.5
SO2570	Putative lipoprotein (3)	1.0	58.3	34	54.5	26.5	10	6
SO2682	Hypothetical protein (9)	2.5	54.5	3	7	0.0	0	0
SO2766	Conserved hypothetical protein (9)	1.0	63.6	27	25.5	34.3	7	6
SO2882	Conserved hypothetical protein (9)	0.80	75.2	51	91.5	43.8	21	23
SO2893	Conserved hypothetical protein (9)	1.9	72.3	16	57	25.1	3	4.5
SO2991	Conserved hypothetical protein (9)	0.70	55.0	5	10	0.0	0	0
SO3030	Siderophore biosynthesis protein, AlcA (17)	1.6	60.8	27	79.5	36.7	10	9.5
SO3069	Conserved hypothetical protein (9)	1.6	31.2	30	44.5	10.8	7	7
SO3103	AcrB/AcrD/AcrF family protein (4)	1.1	34.1	23	22.5	13.7	9	6.5
SO3145	Electron transfer flavoprotein, beta subunit, EtfB (7)	1.2	96.4	26	131.5	64.3	14	45.5
SO3207	Chemotaxis protein (4)	1.5	54.9	44	127	46.7	24	32
SO3235	Flagellar hook-associated protein FliD (4)	0.80	71.3	30	39	34.6	7	5.5
SO3247	Flagellar hook protein FlgE (4)	0.90	66.0	14	36.5	31.1	6	10
SO3314	Putative fimbrial biogenesis and twitching motility protein (4)	1.0	53.1	10	10.5	0.0	0	0
SO3343	Conserved hypothetical protein (9)	0.80	81.2	20	97.5	61.3	11	28
SO3407	Conserved hypothetical protein (9)	0.80	28.6	16	16	0.0	0	0
SO3422	Ribosomal subunit interface protein, YfiA-2 (12)	1.0	89.8	8	28	17.8	2	1
SO3433	Lipoprotein NlpD (3)	1.2	46.3	10	9.5	0.0	0	0
SO3434	Protein-L-isoaspartate O-methyltransferase, Pcm (11)	0.80	64.0	9	7.5	0.0	0	0
SO3442	MazG family protein (18)	1.6	66.3	13	26	18.6	3	3.5
SO3468	Riboflavin synthase, alpha subunit, RibE-2 (2)	1.1	51.8	10	11	0.0	0	0
SO3483	HlyD family secretion protein (17)	1.0	68.6	19	18.5	25.5	5	3
SO3516	Transcriptional regulator, LacI family (14)	1.2	49.1	13	14	15.7	3	3
SO3539	Peptidase, M28D family (11)	0.50	72.7	26	40	30.7	9	5
SO3550	Hypothetical protein (9)	1.0	57.4	9	7	0.0	0	0
SO3560	Peptidase, M16 family (11)	0.30	65.0	45	50	33.7	20	19
SO3565	2,3-Cyclic-nucleotide 2-phosphodiesterase, CpdB (13)	0.70	79.7	53	74.5	28.8	12	8.5
SO3597	Conserved hypothetical protein (9)	1.0	78.7	13	48	0.0	0	0
SO3683	Coniferyl aldehyde dehydrogenase (7)	0.50	55.1	24	33	21.1	6	6.5
SO3720	Conserved hypothetical protein (9)	1.6	80.1	12	21.5	29.8	4	2.5
SO3800	Serine protease, subtilase family (11)	0.50	19.7	11	7	0.0	0	0
SO3936	Sodium-type flagellar protein MotX (17)	0.90	47.6	8	6	0.0	0	0
SO3969	OmpA family protein (3)	1.5	61.8	14	19.5	20.6	2	1.5
SO3980	Cytochrome c_{552} nitrite reductase (7)	1.2	49.5	27	49.5	20.3	7	6.5
SO4319	HlyD family secretion protein (17)	1.3	46.7	20	23	25.0	7	6
SO4329	Conserved hypothetical protein (9)	1.4	94.0	15	47	66.7	6	13
SO4403	Hypothetical protein (9)	0.50	72.5	16	18	22.1	2	2
SO4505	Conserved hypothetical protein (9)	0.50	80.7	8	11.5	0.0	0	0
SO4523	Iron-regulated outer membrane virulence protein IrgA (17)	0.60	78.9	55	169	48.3	23	36.5
SOA0110	Putative lipoprotein (3)	0.50	43.3	10 (46)	147	16.4	1 (16)	32
SOA0112	Putative lipoprotein (3)	NA[e]	47.7	0 (52)	224.5	20.4	0 (17)	31.5

[a] Relative gene expression (induction) is presented as the mean ratio of the fluorescence intensity of Cr(VI)-exposed cells (experimental) to control (nonexposed) cells.
[b] Total sequence coverage from replicate analyses.
[c] Total number of unique peptides identified per protein from replicate analyses.
[d] Average number of spectra identified per protein from replicate analyses.
[e] NA, not applicable; gene was not represented on the microarray.
[f] From Table 1.

tions (Tables 2 and 3). Located immediately upstream of *nlpD* (SO3433) in the MR-1 chromosome is the gene *pcm*, which is predicted to encode protein-L-isoaspartate *O*-methyltransferase, an enzyme involved in protein modification and repair. The ORF coding for the RNA polymerase sigma factor RpoS,

which controls the expression of many stationary-phase-induced genes, is positioned just downstream of *nlpD* and is transcribed in the same direction as *nlpD* and *pcm*. Proteomic analysis revealed that, in addition to the lipoprotein NlpD, expression of protein-L-isoaspartate *O*-methyltransferase was

downregulated under conditions of 24-h Cr(VI) exposure (Table 3). This is of interest because, with age or under stress conditions, proteins are susceptible to various spontaneous or deleterious covalent modifications such as deamidation, the conversion of asparagines into aspartyls and isoaspartyls, which can result in loss of protein function. Pcm functions in repairing damaged proteins by selectively methylating atypical L-isoaspartyl sites and converting them back to L-aspartyls (5, 33). The enzyme was shown to enhance the survival of stationary-phase *E. coli* subjected to a secondary environmental stress (58). The physiological significance of decreased synthesis of *S. oneidensis* Pcm under the Cr(VI) conditions used here is unclear.

Genes and proteins involved in DNA metabolism. Chromate and its derivatives have been shown to cause Cr-DNA adducts and DNA-DNA cross-links (11, 27, 28, 43, 47, 53, 59, 64, 65), which can disrupt regulation of gene expression or change DNA topology, leading to altered cell function and perhaps even cell death. Cr(III) can cause DNA damage and negatively affect DNA topology by directly inhibiting topoisomerase DNA relaxation activity (40). Five of the 56 upregulated proteins detected by HPLC-MS/MS under conditions of 24-h Cr(VI) exposure had predicted functions related to DNA metabolism: site-specific recombinase (SO3013), DNA topoisomerase III (TopB, SO3061), type I restriction-modification system subunit (HsdM-2, SO4265), type II restriction endonuclease (SOA0003), and type II DNA modification methyltransferase (SOA0004) (Table 2). At the transcription level, we observed the low-level induction of three genes annotated as helicase genes in response to Cr(VI) conditions: SO0368 (encoding helicase; 1.7-fold), *uvrD* (encoding DNA helicase II; 2.1-fold), and *hrpA* (encoding ATP-dependent helicase; 2.1-fold) (see supplemental Table S1 at http://compbio.ornl.gov/shewanella_metal_stress /chronic/supplemental). DNA helicases catalyze the unwinding of energetically stable duplex DNA and, as a result, play important roles in nearly all aspects of DNA metabolism, including replication, recombination, repair, and transcription (reviewed in reference 54). Additionally, *recO*, which encodes DNA repair protein RecO, was upregulated twofold under conditions of prolonged Cr(VI) challenge. DNA helicases in *Pseudomonas aeruginosa* have been implicated in chromate resistance via their involvement in repairing DNA damage (31) and perhaps play a similar role in Cr(VI)-stressed *S. oneidensis*.

Expression of energy metabolism genes. Many facultative anaerobic bacteria synthesize specific primary dehydrogenases and terminal reductases or oxidases as a mechanism for appropriately adapting their respiratory electron-transport chains to environmental changes (45). Sequence analysis of the MR-1 genome revealed extensive duplication of genes involved in electron transport (23). These genes no doubt are important in the ability of *S. oneidensis* to function as a "respiratory generalist" (23) by allowing MR-1 to adapt to specific growth conditions.

Under our chromate treatment conditions, 9 of the 13 *nuo* genes (SO1009 to SO1021) encoding subunits of the heteromultimeric NADH dehydrogenase I were upregulated, as identified by microarray analysis: *nuoCD*, 2.5-fold; *nuoE*, 2.8-fold; *nuoF*, 4.4-fold; *nuoG*, 3.1-fold; *nuoI*, 4.1-fold; *nuoJ*, 6.0-fold; *nuoL*, 3.7-fold; *nuoM*, 6.1-fold; *nuoN*, 3.5-fold (see supplemental Table S1 at http://compbio.ornl.gov/shewanella_metal_stress

/chronic/supplemental). Transcripts for the other four *nuo* genes (i.e., *nuoA*, *nuoB*, *nuoH*, and *nuoK*) either showed decreased abundance under Cr(VI) conditions or failed to meet our criterion of at least a twofold change in expression. None of the NADH dehydrogenase subunits were found to be differentially expressed at the protein level. Additionally, we observed a two- to fivefold induction of genes encoding ubiquinol-cytochrome *c* reductase (*petC*, SO0610), tetraheme cytochrome *c* (SO3056), and cytochrome *d* ubiquinol oxidase (*cydA*, SO3286) under conditions of 24-h Cr(VI) exposure (see supplemental Table S1). The *S. oneidensis* oxidase-encoding gene *cydA* also was shown to be induced during Cr(VI) reduction in another study (7). Preliminary growth and reduction studies of an MR-1 strain harboring an in-frame deletion of *petC* indicated that the mutant showed severe growth deficiency compared to wild-type MR-1 under aerobic conditions in the presence of 0.3 mM chromate (S. Barua and K. Chourey, unpublished data).

Five proteins with annotated functions in energy metabolism were identified as being downregulated under chronic Cr(VI) conditions: NADH:ubiquinone oxidoreductase, alpha subunit (NqrA-1); alanine dehydrogenase (Ald); electron transfer flavoprotein, beta subunit (EtfB); coniferyl aldehyde dehydrogenase (SO3683); and cytochrome c_{552} nitrite reductase (SO3980) (Table 3). Two of these downregulated proteins (NqrA-1 and EtfB) are involved in electron transport processes. The transcriptomic and proteomic data suggest that *S. oneidensis* modulates expression of electron transport chain components in response to environmental signals (i.e., growth conditions), resulting in the coexistence of a certain subset of dehydrogenases and reductases/oxidases under environmental Cr(VI) conditions.

Thioredoxins, which have a dithiol/disulfide active site (CGPC), comprise part of a ubiquitous disulfide-reducing system that is involved in a number of important cellular functions, including maintenance of the intracellular redox state and redox regulation of protein function, defense against oxidative stress, and prevention of disulfide bond formation, and function as efficient oxidoreductases of disulfides (for a review, see reference 4). Glutaredoxins catalyze the reduction of disulfides via reduced glutathione in a reaction coupled to glutathione reductase and NADPH. Chromate toxicity is associated with the intracellular reduction of Cr(VI) to lower oxidation states, a process that generates free radicals and imposes oxidative damage on DNA (16). In response to prolonged Cr(VI) exposure, two putative thioredoxin-coding transcripts (SO0476 and SO3117) were upregulated two- to threefold, whereas a gene (SO2100) encoding a thioredoxin family protein was downregulated under the same growth conditions (see supplemental Table S1 at http://compbio.ornl .gov/shewanella_metal_stress/chronic/supplemental). *S. oneidensis* glutaredoxin (SO2745) also was transcriptionally induced by 6.9-fold under Cr(VI) stress. Other investigators have demonstrated that, while thioredoxin protein products are partially redundant in terms of biochemical function, their gene expression can be differentially regulated depending on the type of stressor (32).

Downregulation of transport, motility, and chemotaxis genes and proteins. The vast majority of MR-1 proteins downregulated under our experimental conditions are annotated as hypotheticals (Table 1). Besides poorly characterized proteins, other downregulated proteins belonged to the functional cat-

egories of cellular process proteins, transport and binding proteins, cell envelope proteins, and energy metabolism proteins. The relative abundance levels of seven proteins were found to be decreased under 24-h Cr(VI) exposure compared to the control conditions: two chemotaxis proteins (SO1144 and SO3207), a cation transport ATPase (SO1689), an AcrB/AcrD/AcrF family protein (SO3103), and three proteins involved in motility (FliD, FlgE, and SO3314) (Table 3). Downregulation of proteins involved in motility and chemotaxis was consistent with confocal laser scanning microscopy observations, which indicated a prevalence of nonmotile cells under prolonged Cr(VI) exposure (data not shown). Additional chemotaxis genes displayed transcriptional repression under Cr stress and included *cheY1* (0.4-fold), *cheA* (0.5-fold), *cheW* (0.3-fold), and *cheB1* (0.5-fold) (see supplemental Table S1 at http://compbio.ornl.gov/shewanella_metal_stress/chronic/supplemental).

Our previous work showed that a major feature characterizing the *S. oneidensis* response to acute chromate stress was the high induction of genes encoding components of a TonB1 iron transport system (*tonB1-exbB1-exbD1*), hemin ATP-binding cassette (ABC) transporters (*hmuTUV*), and various outer membrane TonB-dependent receptors (14). Almost one-half of the proteins upregulated under chromate shock were predicted to have transport and binding functions. Prolonged exposure to Cr(VI) elicited a very different molecular response. In general, iron sequestration and other transport/binding genes were either repressed in response to 24-h Cr(VI) exposure or induced at substantially lower levels. Genes encoding a heme transport protein (*hugA*; 0.50-fold) and a TonB1 protein (*tonB1*; 0.30-fold), for example, were downregulated under the Cr(VI) conditions used in this study, in contrast to the 120- and 99-fold inductions, respectively, observed in response to a 90-min acute exposure (14) (see supplemental Table S1 at http://compbio.ornl.gov/shewanella_metal_stress/chronic/supplemental). Both AlcA (SO3030, a siderophore biosynthesis protein) and IrgA (SO4523, an iron-regulated outer membrane virulence protein) were upregulated under acute chromate stress (14) but were downregulated in response to a 24-h exposure (Table 3). Additionally, both *bfr-1* and *bfr-2*, encoding bacterioferritin subunits 1 and 2, respectively, were downregulated twofold under our Cr(VI) treatment conditions but were shown to be upregulated during active Cr(VI) reduction by Bencheikh-Latmani et al. (7).

Genes involved in phosphate transport also were downregulated. This was observed only at the transcript level with the repression of two distinct gene clusters with annotated functions in phosphate assimilation: (i) the first cluster (SO1723 to -26) is composed of three genes encoding phosphate ABC transporters (SO1723, 0.30-fold; SO1724, 0.30-fold; *pstB1*, 0.40-fold) and *phoU* (0.50-fold), a regulatory gene for phosphate transport that is involved in downregulating the phosphate (Pho) regulon under conditions of excess phosphate; (ii) a second gene cluster (SO1557 to -60) encodes a putative outer membrane porin (SO1557, 0.30-fold), PhoB (SO1558, 0.30-fold), PhoR (SO1559, 0.40-fold), and a phosphate-binding protein (SO1560, 0.20-fold) (see supplemental Table S1 at http://compbio.ornl.gov/shewanella_metal_stress/chronic/supplemental). The outer membrane porin (SO1557) may play a role in phosphate uptake. The signal-transducing proteins of the PhoB-PhoR two-component regulatory system are required for transcriptional activation of the *E. coli* Pho regulon in response to external inor-

ganic phosphate limitation (reviewed in reference 62). Some of these genes, namely, SO1557, *phoB*, and SO1723, were observed to be repressed as well in response to anaerobic Cr(VI)-reducing conditions (7). Other transporter genes displaying repression included SO0986 (0.50-fold) for chromate transport and several efflux family genes (SO1918, SO2045, and SOA0159) for multidrug and cation transport. Similarly, gene SO0986, encoding a putative chromate transporter, was not found to be upregulated under anaerobic Cr(VI)-reducing conditions (7).

Conclusion. Combined transcriptomic and proteomic analyses provided a global view of the molecular response induced upon 24-h Cr(VI) challenge of *S. oneidensis* MR-1. Analytical assays indicated the complete disappearance of Cr(VI) from the growth medium at the 24-h time point of exposure, when cells were harvested for analysis, suggesting the intracellular accumulation of chromate and/or its derivatives. As revealed by integrated transcriptome and proteome analyses, the predominant molecular response of MR-1 to 24-h Cr(VI) challenge was the strong upregulation of numerous prophage-related (LambdaSo, MuSo1, and MuSo2) genes, suggesting that prophage activation may be the primary factor leading to cell lysis under these environmental conditions. These findings were in marked contrast to our previous global examination of the MR-1 temporal response to an acute treatment of 1 mM chromate over a 90-min period (14). Other differences in the gene and protein expression profiles included the downregulation or low-level induction (two- to fourfold) of genes encoding iron binding and transport functions (e.g., putative operons *alcA*-SO3031-SO3032, *tonB1-exbB1-exbD1*, *hmuTUV*), a DNA-binding response regulator (SO2426), and a putative azoreductase (SO3585) under 24-h Cr(VI) exposure (see supplemental Tables S1 and S2 at http://compbio.ornl.gov/shewanella_metal_stress/chronic/supplemental), whereas these genes and their corresponding proteins were upregulated at high expression levels (in some cases, >50-fold) in response to an acute chromate challenge (14). Transcriptional induction of cell wall biosynthesis and cell division genes (i.e., the putative *mur* and *fts* operon), as well as *rodA*, *mreD*, and *era*, appeared to correlate with the extreme filamentous morphology observed using confocal microscopy and AFM topographic imaging. The induction of genes encoding molecular chaperones, classical heat shock proteins, oxidative stress protection proteins, thioredoxins, and glutaredoxins correlated with the susceptibility of *S. oneidensis* MR-1 to prolonged Cr(VI) exposure.

REFERENCES

1. **Abboud, R., R. Popa, V. Souza-Egipsy, C. S. Giometti, S. Tollaksen, J. J. Mosher, R. H. Findlay, and K. H. Nealson.** 2005. Low-temperature growth of *Shewanella oneidensis* MR-1. Appl. Environ. Microbiol. **71:**811–816.

2. **Ackerley, D. F., Y. Barak, S. V. Lynch, J. Curtin, and A. Matin.** 2006. Effect of chromate stress on *Escherichia coli* K-12. J. Bacteriol. **188:**3371–3381.

3. **Alvarez, A. H., R. Moreno-Sanchez, and C. Cervantes.** 1999. Chromate efflux by means of the ChrA chromate resistance protein from *Pseudomonas aeruginosa.* J. Bacteriol. **181:**7398–7400.

4. **Arner, E. S. J., and A. Holmgren.** 2000. Physiological functions of thioredoxin and thioredoxin reductase. Eur. J. Biochem. **267:**6102–6109.

5. **Aswad, D. W.** 1984. Stoichiometric methylation of porcine adrenocorticotropin by protein carboxyl methyltransferase requires deamidation of asparagine 25. Evidence for methylation at the alpha-carboxyl group of atypical L-isoaspartyl residues. J. Biol. Chem. **259:**10714–10721.

6. **Beliaev, A. S., D. M. Klingeman, J. A. Klappenbach, L. Wu, M. F. Romine, J. M. Tiedje, K. H. Nealson, J. K. Fredrickson, and J. Zhou.** 2005. Global transcriptome analysis of *Shewanella oneidensis* MR-1 exposed to different terminal electron acceptors. J. Bacteriol. **187:**7138–7145.

7. **Bencheikh-Latmani, R., S. M. Williams, L. Haucke, C. S. Criddle, L. Wu, J. Zhou, and B. M. Tebo.** 2005. Global transcriptional profiling of *Shewanella oneidensis* MR-1 during Cr(VI) and U(VI) reduction. Appl. Environ. Microbiol. **71:**7453–7460.

8. **Bi, E. F., and J. Lutkenhaus.** 1991. FtsZ ring structure associated with division in *Escherichia coli.* Nature **354:**161–164.

9. **Bopp, L. H., A. M. Chakrabarty, and H. L. Ehrlich.** 1983. Chromate resistance plasmid in *Pseudomonas fluorescens.* J. Bacteriol. **155:**1105–1109.

10. **Braga, P. C., and D. Ricci.** 1998. Atomic force microscopy: application to investigation of *Escherichia coli* morphology before and after exposure to cefodizime. Antimicrob. Agents Chemother. **42:**18–22.

11. **Bridgewater, L. C., F. C. R. Manning, E. S. Woo, and S. R. Patierno.** 1994. DNA polymerase arrest by adducted trivalent chromium. Mol. Carcinog. **9:**122–133.

12. **Britton, R. A., B. S. Powell, S. Dasgupta, Q. Sun, W. Margolin, J. R. Lupski, and D. L. Court.** 1998. Cell cycle arrest in Era GTPase mutants: a potential growth rate-regulated checkpoint in *Escherichia coli.* Mol. Microbiol. **27:**739–750.

13. **Brown, S. D., M. Martin, S. Deshpande, S. Seal, K. Huang, E. Alm, Y. Yang, L. Wu, T. Yan, X. Liu, A. Arkin, K. Chourey, J. Zhou, and D. K. Thompson.** 2006. Cellular response of *Shewanella oneidensis* to strontium stress. Appl. Environ. Microbiol. **72:**890–900.

14. **Brown, S. D., M. R. Thompson, N. C. VerBerkmoes, K. Chourey, M. Shah, J. Zhou, R. L. Hettich, and D. K. Thompson.** 2006. Molecular dynamics of the *Shewanella oneidensis* response to chromate stress. Mol. Cell. Proteomics **5:**1054–1071.

15. **Buddelmeijer, N., and J. Beckwith.** 2002. Assembly of cell division proteins at the *E. coli* cell center. Curr. Opin. Microbiol. **5:**553–557.

16. **Cervantes, C., J. Campos-García, S. Devars, F. Gutiérrez-Corona, H. Loza-Tavera, J. C. Torres-Guzmán, and R. Moreno-Sánchez.** 2001. Interactions of chromium with microorganisms and plants. FEMS Microbiol. Rev. **25:**335–347.

17. **Cervantes, C., and H. Ohtake.** 1988. Plasmid-determined resistance to chromate in *Pseudomonas aeruginosa.* FEMS Microbiol. Lett. **56:**173–176.

18. **Cervantes, C., H. Ohtake, L. Chu, T. K. Misra, and S. Silver.** 1990. Cloning, nucleotide sequence, and expression of the chromate resistance determinant of *Pseudomonas aeruginosa* plasmid pUM505. J. Bacteriol. **172:**287–291.

19. **Cooper, S.** 1991. Bacterial growth and division. Academic Press, Inc., San Diego, Calif.

20. **Gao, H., Y. Wang, X. Liu, T. Yan, L. Wu, E. Alm, A. Arkin, D. K. Thompson, and Z. Zhou.** 2004. Global transcriptome analysis of the heat shock response of *Shewanella oneidensis.* J. Bacteriol. **186:**7796–7803.

21. **Gollop, N., and P. E. March.** 1991. A GTP-binding protein (Era) has an essential role in growth rate and cell cycle control in *Escherichia coli.* J. Bacteriol. **173:**2265–2270.

22. **Guzman, L. M., D. S. Weiss, and J. Beckwith.** 1997. Domain-swapping analysis of FtsI, FtsL, and FtsQ, bitopic membrane proteins essential for cell division in *Escherichia coli.* J. Bacteriol. **179:**5094–5103.

23. **Heidelberg, J. F., I. T. Paulsen, K. E. Nelson, E. J. Gaidos, W. C. Nelson, T. D. Read, J. A. Eisen, R. Seshadri, N. Ward, B. Methe, R. A. Clayton, T. Meyer, A. Tsapin, J. Scott, M. Beanan, L. Brinkac, S. Daugherty, R. T. DeBoy, R. J. Dodson, A. S. Durkin, D. H. Haft, J. F. Kolonay, R. Madupu, J. D. Peterson, L. A. Umayam, O. White, A. M. Wolf, J. Vamathevan, J. Weidman, M. Impraim, K. Lee, K. Berry, C. Lee, J. Mueller, H. Khouri, J. Gill, T. R. Utterback, L. A. McDonald, T. V. Feldblyum, H. O. Smith, J. C. Venter, K. H. Nealson, and C. M. Fraser.** 2002. Genome sequence of the dissimilatory metal ion-reducing bacterium *Shewanella oneidensis.* Nat. Biotechnol. **20:**1118–1123.

24. **Hu, P., E. L. Brodie, Y. Suzuki, H. H. McAdams, and G. L. Andersen.** 2005. Whole-genome transcriptional analysis of heavy metal stresses in *Caulobacter crescentus.* J. Bacteriol. **187:**8437–8449.

25. **James, B. R.** 1996. The challenge of remediating chromium-contaminated soil. Environ. Sci. Technol. **30:**A248–A251.

26. **Langard, S.** 1980. Chromium, p. 111–132. *In* H. A. Waldron (ed.), Metals in the environment. Academy Press Inc., New York, N.Y.

27. **Liu, S., and K. Dixon.** 1996. Induction of mutagenic DNA damage by chromium(VI) and glutathione. Environ. Mol. Mutagen. **28:**71–79.

28. **Mattagajasingh, S. N., and H. P. Misra.** 1999. Analysis of EDTA-chelatable proteins from DNA-protein cross-links induced by a carcinogenic chromium(VI) in cultured intact human cells. Mol. Cell. Biochem. **199:**146–162.

29. **McDonald, W. H., R. Ohi, D. T. Miyamoto, T. J. Mitchison, and J. R. Yates III.** 2002. Comparison of three directly coupled HPLC MS/MS strategies for identification of proteins from complex mixtures: single-dimension LC-MS/MS, 2-phase MudPIT, and 3-phase MudPIT. Int. J. Mass Spectrom. **219:**245–251.

30. **Middleton, S. S., R. B. Latmani, M. R. Mackey, M. H. Ellisman, B. M. Tebo, and C. S. Criddle.** 2003. Cometabolism of Cr(VI) by *Shewanella oneidensis* MR-1 produces cell-associated reduced chromium and inhibits growth. Biotechnol. Bioeng. **83:**627–637.

31. **Miranda, A. T., M. V. Gonzalez, G. Gonzalez, E. Vargas, J. Campos-Garcia, and C. Cervantes.** 2005. Involvement of DNA helicases in chromate resistance by *Pseudomonas aeruginosa* PAO1. Mutat. Res. **578:**202–209.

32. **Missall, T. A., and J. K. Lodge.** 2005. Function of the thioredoxin proteins in *Cryptococcus neoformans* during stress or virulence and regulation by putative transcriptional modulators. Mol. Microbiol. **57:**847–858.

33. **Murray, E. D., Jr., and S. Clarke.** 1984. Synthetic peptide substrates for the erythrocyte protein carboxyl methyltransferase. Detection of a new site of methylation at isomerized L-aspartyl residues. J. Biol. Chem. **259:**10722–10732.

34. **Myers, C. R., B. P. Carstens, W. E. Antholine, and J. M. Myers.** 2000. Chromium(VI) reductase activity is associated with the cytoplasmic membrane of anaerobically grown *Shewanella putrefaciens* MR-1. J. Appl. Microbiol. **88:**98–106.

35. **Myers, C. R., and K. H. Nealson.** 1988. Bacterial manganese reduction and growth with manganese oxide as the sole electron acceptor. Science **240:**1319–1321.

36. **Nies, A., D. H. Nies, and S. Silver.** 1989. Cloning and expression of plasmid genes encoding resistance to chromate and cobalt in *Alcaligenes eutrophus.* J. Bacteriol. **171:**5065–5070.

37. **Nies, A., D. H. Nies, and S. Silver.** 1990. Nucleotide sequence and expression of a plasmid-encoded chromate resistance determinant from *Alcaligenes eutrophus.* J. Biol. Chem. **265:**5648–5653.

38. **Ohtake, H., C. Cervantes, and S. Silver.** 1987. Decreased chromate uptake in *Pseudomonas fluorescens* carrying a chromate resistance plasmid. J. Bacteriol. **169:**3853–3856.

39. **Park, C. H., M. Keyhan, B. Wielinga, S. Fendorf, and A. Matin.** 2000. Purification to homogeneity and characterization of a novel *Pseudomonas putida* chromate reductase. Appl. Environ. Microbiol. **66:**1788–1795.

40. **Plaper, A., S. Jenko-Brinovec, A. Premzl, J. Kos, and P. Raspor.** 2002. Genotoxicity of trivalent chromium in bacterial cells. Possible effects on DNA topology. Chem. Res. Toxicol. **15:**943–949.

41. **Qiu, X., M. J. Daly, A. Vasilenko, M. V. Omelchenko, E. K. Gaidamakova, L. Wu, J. Zhou, G. W. Sundin, and J. M. Tiedje.** 2006. Transcriptome analysis applied to survival of *Shewanella oneidensis* MR-1 exposed to ionizing radiation. J. Bacteriol. **188:**1199–1204.

42. **Qiu, X., G. W. Sundin, L. Wu, J. Zhou, and J. M. Tiedje.** 2005. Comparative analysis of differentially expressed genes in *Shewanella oneidensis* MR-1 following exposure to UVC, UVB, and UVA radiation. J. Bacteriol. **187:**3556–3564.

43. **Quievryn, G., J. Messer, and A. Zhitkovich.** 2002. Carcinogenic chromium(VI) induces cross-linking of vitamin C to DNA in vitro and in human lung A549 cells. Biochemistry **41:**3156–3167.

44. **Ram, R. J., N. C. VerBerkmoes, M. P. Thelen, G. W. Tyson, B. J. Baker, R. C. Blake II, M. Shah, R. L. Hettich, and J. F. Banfield.** 2005. Community proteomics of a natural microbial biofilm. Science **308:**1915–1920.

45. **Richardson, D. J.** 2000. Bacterial respiration: a flexible process for a changing environment. Microbiology **146:**551–571.

46. **Russo, P., A. Catassi, A. Cesario, A. Imperatori, N. Rotolo, M. Fini, P. Granone, and L. Dominioni.** 2005. Molecular mechanisms of hexavalent chromium-induced apoptosis in human bronchoalveolar cells. Am. J. Respir. Cell Mol. Biol. **33:**589–600.

47. **Salnikow, K., A. Zhitkovich, and M. Costa.** 1992. Analysis of the binding sites of chromium to DNA and protein in vitro and in intact cells. Carcinogenesis **12:**2341–2346.

48. **Schena, M., D. Shalon, R. Heller, A. Chai, P. O. Brown, and R. W. Davis.** 1996. Parallel human genome analysis: microarray-based expression monitoring of 1000 genes. Proc. Natl. Acad. Sci. USA **93:**10614–10619.

49. **Summers, A. O., and G. A. Jacoby.** 1978. Plasmid-determined resistance to boron and chromium compounds in *Pseudomonas aeruginosa.* Antimicrob. Agents Chemother. **13:**637–640.

50. **Suzuki, T., N. Miyata, H. Horitsu, K. Kawai, K. Takamizawa, Y. Tai, and M. Okazaki.** 1992. NAD(P)H-dependent chromium (VI) reductase of *Pseudomonas ambigua* G-1: a Cr(V) intermediate is formed during the reduction of Cr(VI) to Cr(III). J. Bacteriol. **174:**5340–5345.

51. **Thibessard, A., A. Fernandez, B. Gintz, N. Leblond-Bourget, and B. Decaris.** 2002. Effects of *rodA* and *pbp2b* disruption on cell morphology and oxidative stress response of *Streptococcus thermophilus* CNRZ368. J. Bacteriol. **184:**2821–2826.

52. **Thompson, D. K., A. S. Beliaev, C. S. Giometti, S. L. Tollaksen, T. Khare,**

D. P. Lies, K. H. Nealson, H. Lim, J. Yates III, C. C. Brandt, J. M. Tiedje, and J. Zhou. 2002. Transcriptional and proteomic analysis of a ferric uptake regulator (Fur) mutant of *Shewanella oneidensis*: possible involvement of Fur in energy metabolism, transcriptional regulation, and oxidative stress. Appl. Environ. Microbiol. **68:**881–892.

53. Tsapakos, M. J., T. H. Hampton, P. R. Sinclair, J. F. Sinclair, W. J. Bement, and K. E. Wettehahn. 1983. The carcinogen chromate causes DNA damage and inhibits drug-mediated induction of porphyrin accumulation and glucuronidation in chick embryo hepatocytes. Carcinogenesis **4:**959–966.

54. Tuteja, N., and R. Tuteja. 2004. Prokaryotic and eukaryotic DNA helicases. Essential molecular motor proteins for cellular machinery. Eur. J. Biochem. **271:**1835–1848.

55. VerBerkmoes, N. C., M. B. Shah, P. K. Lankford, D. A. Pelletier, M. B. Strader, D. L. Tabb, W. H. McDonald, J. W. Barton, G. B. Hurst, L. Hauser, B. H. Davison, J. T. Beatty, C. S. Harwood, F. R. Tabita, R. L. Hettich, and F. W. Larimer. 2005. Determination and comparison of the baseline proteomes of the versatile microbe *Rhodopseudomonas palustris* under its major metabolic states. J. Proteome Res. **5:**287–298.

56. Viamajala, S., B. M. Peyton, W. A. Apel, and J. N. Petersen. 2002. Chromate/nitrite interactions in *Shewanella oneidensis* MR-1: evidence for multiple hexavalent chromium [Cr(VI)] reduction mechanisms dependent on physiological growth conditions. Biotechnol. Bioeng. **78:**770–778.

57. Vijaranakul, U., M. J. Nadakavukaren, B. L. M. de Jonge, B. J. Wilkinson, and R. K. Jayaswal. 1995. Increased cell size and shortened peptidoglycan interpeptide bridge of NaCl-stressed *Staphylococcus aureus* and their reversal by glycine betaine. J. Bacteriol. **177:**5116–5121.

58. Visick, J. E., H. Cai, and S. Clarke. 1998. The L-isoaspartyl protein repair methyltransferase enhances survival of aging *Escherichia coli* subjected to secondary environmental stresses. J. Bacteriol. **180:**2623–2629.

59. Voitkun, V., A. Zhitkovich, and M. Costa. 1994. Complexing of amino acids to DNA by chromate in intact cells. Environ. Health Perspect. **102:**251–255.

60. Vollmer, W., and J.-V. Höltje. 2001. Morphogenesis of *Escherichia coli*. Curr. Opin. Microbiol. **4:**625–633.

61. Wan, X.-F., N. C. VerBerkmoes, L. A. McCue, D. Stanek, H. Connelly, L. J. Hauser, L. Wu, X. Liu, T. Yan, A. Leaphart, R. L. Hettich, J. Zhou, and D. K. Thompson. 2004. Transcriptomic and proteomic characterization of the Fur modulon in the metal-reducing bacterium *Shewanella oneidensis*. J. Bacteriol. **186:**8385–8400.

62. Wanner, B. L. 1996. Phosphorus assimilation and control of the phosphate regulon, p. 1357–1381. *In* F. C. Neidhardt, R. Curtiss III, J. L. Ingraham, E. C. C. Lin, K. B. Low, B. Magasanik, W. S. Reznikoff, M. Riley, M. Schaechter, and H. E. Umbarger (ed.), *Escherichia coli* and *Salmonella*: cellular and molecular biology. ASM Press, Washington, D.C.

63. Weiss, D. S. 2004. Bacterial cell division and the septal ring. Mol. Microbiol. **54:**588–597.

64. Xie, H., S. S. Wise, A. L. Holmes, B. Xu, T. P. Wakeman, S. C. Pelsue, N. P. Singh, and J. P. Wise, Sr. 2005. Carcinogenic lead chromate induces DNA double-strand breaks in human lung cells. Mutat. Res. **586:**160–172.

65. Zhitkovich, A., V. Voitkun, and M. Costa. 1995. Glutathione and free amino acids form stable complexes with DNA following exposure of intact mammalian cells to chromate. Carcinogenesis **16:**907–913.